Colocalization-NTA of multi-stained platelet derived MSC-EV preparations

Particle Metrix GmbH, Inning, Germany
Institute for Transfusion Medicine (AG Giebel), University Hospital Essen,
University of Duisburg-Essen, Germany

Abstract

Colocalization Nanoparticle Tracking Analysis (C-NTA) represents significant further development of fluorescence-NTA (F-NTA) methods. In addition to measuring the size and concentration of fluorescently labelled particles, C-NTA offers the ability to quickly detect two or more fluorescently labelled targets which coincide on a single extracellular vesicle. Multiple lasers and the selection of corresponding fluorescence filters allow for quantification of individual fluorescent sub-populations as well as particles which are double-positive for different surface markers.

After successfully showing C-NTA of double-stained MSC-EVs in our previous study (https://bit.ly/43GG0Yk) and confirming the results with image flow cytometry, this note describes C-NTA of multi-stained MSC-EVs using a PMX-430 QUATT NTA system with four lasers.

Keywords: colocalization, multi-staining, Nanoparticle Tracking Analysis (NTA), extracellular vesicles, CD41, CD9, CellMask Deep Red, antibody, fluorescence, membrane, NP-40

Introduction

Extracellular vesicles (EVs) from selected cell types are currently being studied intensively because of their critical therapeutic potential. EVs can be classified according to their origin, yet recent studies indicate a high degree of heterogeneity even within certain EV classes [1-6]. One primary goal in EV research is to establish and define methods which facilitate the robust detection of heterogeneity within purified samples of EVs, particularly in sample fractions containing EV sizes < 200 nm [1, 3]; however, progress in this context is still hampered by the fact that most currently available methods for analysing smaller EVs are either very time consuming or can only quantify a limited set of parameters [7, 8].

C-NTA, derived from F-NTA methods, allows the measurement of targeted biomarker detection by capturing multiple fluorescence signals from different EV phenotypes in one sample, as well as revealing biomarker coincidence at the single vesicle level, all in a single rapid measurement.

This note is a follow-up to our previous study (https://bit.ly/43GG0Yk) in which we described C-NTA experiments on double-stained human platelet lysate-derived mesenchymal stem cell EVs. In this paper, MSC-EVs were multi-stained with the membrane dye CellMask™ Deep Red (CMDR) and with anti-CD9 and anti-CD41 antibodies conjugated to Pacific Blue and Alexa Fluor™ 488, respectively. A significant fraction of double-positive EVs was detected and quantified in each pair of C-NTA channels. Further, we show that the sequence of antibody/dye stain preparation does not affect the measured colocalization ratios.

Methods

Cell culture and purification of MSC-EVs:

EVs were derived from MSC conditioned media grown

in the presence of human platelet-lysate *via* a PEG precipitation procedure [see previous study 15, 16].

Fluorescence labelling:

For antibody labelling, a cocktail of (i) 1 µl of MSC-EVs with a measured concentration of $4.2x10^{11}$ EV/ml, was mixed with (ii) 5 µl of a 1:25 dilution of anti-Hu CD9PB, a Pacific Blue-conjugated antibody (clone MEM-61), (iii) 5 µl of a 1:125 dilution of anti-Hu CD41-AF488 antibody (clone MEM-06), and (iv) 1 µl of a 1:250 dilution of CMDR Plasma Membrane Stain. Both pre-labeled antibodies were obtained from EXBIO, Vestec (Czech Republic), whereas, CMDR was obtained from Thermo Fisher Scientific (Schwerte, Germany). EVs and both antibodies were incubated for 1 hour in the dark at room temperature. After antibody incubation, CMDR was then added and further incubated for an additional hour, resulting in 2 hours incubation. The incubation cocktail was then diluted with PBS buffer to a final volume of 1 ml for subsequent NTA analyses.

Detergent controls were prepared with non-ionic detergent NP-40 Alternative (*aka* NP-40), from Calbiochem, Merck, Darmstadt (Germany), used to rupture the membrane of EVs. Following incubation, 12 µl of 0.5% NP-40 solution (diluted in particle-free PBS) was added to the labeled EV cocktail, resulting in a final concentration of 0.25% NP-40, and then incubated an additional 30 minutes at room temperature in the dark. The lysed cocktail was diluted into 1 ml of PBS for NTA analyses.

NTA and Colocalization measurements:

NTA measurements of size and concentration as well as colocalization measurements were made with a ZetaView® PMX-430 QUATT equipped with the Particle Metrix Software Suite and the ZetaNavigator software v1.1 (SOPs in Table 1). Measurements and the calculation of the colocalization ratios were performed as described in our previous study (see abstract link). The main difference in this study is that 3 pairs of fluorescence channels (using 405, 488, 640 sources) were used instead of one pair (488 & 640) for determining the colocalization ratios of the EVs.

Table 1: Measurement parameters used for colocalization measurements on a PMX-430 QUATT ZetaView® model

Measurement parameters	Fluorescence mode for anti-CD9 Pacific Blue (λ=405F410nm)	Fluorescence mode for anti-CD41 AF488 (λ=488F500nm)	Fluorescence mode for CellMask™ Deep Red (λ=640F660nm)
Positions	3	3	3
#Cycles	1	1	1
Number of frames	50	50	50
Sensitivity	90	90	90
Shutter	100	200	300
Tracelength	12	12	12
MinArea	0	0	0
MaxArea	1000	1000	1000
MinSize	1	1	1
MaxSize	1000	1000	1000
Framerate	30 fps	30 fps	30 fps
Link Radius	15	15	15
Switch frame	10	10	10
Laser off Frames	5	5	5
Max Skip	1	1	1

Results & Conclusions

Size and concentration measurements:

Standard NTA measurements in scatter mode with the ZetaView® system resulted in a median diameter (X50) of 117 nm and a concentration of $2.5x10^{11}$ particles per ml.

To specifically phenotype EVs in the sample, the particles were multi-labelled with anti-CD9 on Pacific Blue, anti-CD41 on AF488 and the membrane dye CellMask™ Deep Red. The specific choice of fluorochromes reflects our need to ensure that spill-over in the individual fluorescence channels would be avoided.

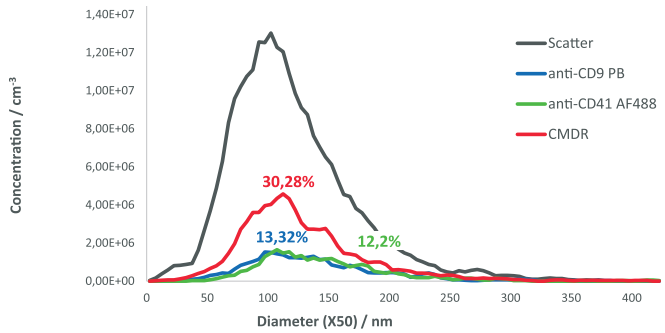

Figure 1: Particle size histograms of MSC-EVs measured in scatter (grey) and fluorescence mode - blue, green and red lines for anti-CD9 Pacific Blue, anti-CD41 AF488 and CellMask™ Deep Red F-NTA detections, respectively.

C-NTA measurements from all three labels yielded dual-positive detections of vesicles in all three pairings of fluorescence channels with the ZetaView® instrument.

CD9-positive EVs resulted in a median diameter (X50) of 128.8 nm and a measured concentration of $3.3x10^{10}$ EV/ml. In contrast, the mean diameter of the CD41-positive EVs was 136.6 nm, which was slightly larger than the particles detected in the other fluorescence and scatter mode. The measured concentration of CD41-positive EVs was $3.05x10^{10}$ EV/ml. EVs positive for CMDR revealed a median size of 124.8 nm and a concentration of $7.57x10^{10}$ particles/ml. This concentration is more than twice as large as the CD9 & CD41 populations, suggesting the presence of additional EVs and/or other lipid-membrane bearing particles without these tetraspanins.

The percentage of CD9- and CD41- and CMDR-positive EVs detected in the blue, green and red fluorescence channels were found to be 13.3%, 12.2% and 30.28%, respectively. Given that the sample was not purified and therefore likely contains different nanoparticles besides EVs, the CMDR results were expected, as this dye does not specifically stain EVs, rather, other lipid- or membrane-containing structures will also be counted in the 640 nm channel.

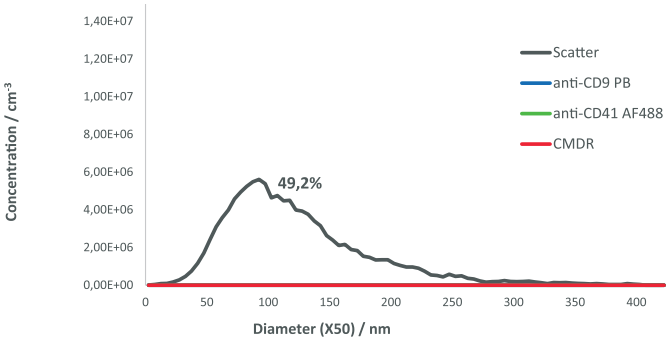

Figure 2: Size distribution of multi-stained EVs after treatment with 0.5% NP-40 for disrupting membranous particles.

NP-40 detergent controls showed a particle number reduced by 50.8% in scatter mode and no particles in the fluorescence mode. The fact that around 50% of the particles remain observable in the scatter mode indicates that half of the population in the sample contains non-membranous particles resistant to the detergent.

Colocalization studies:

Using C-NTA, the same volume of fluorescently labelled particles is illuminated very quickly, one laser after the other with three different wavelengths, and the fluorescence signals are detected in series using the corresponding filters (see table 1). C-NTA of the multi-stained EVs showed colocalization ratios between 39%-41% (see figure 3 A-C) and revealed probably the highest specificity on the vesicles detected for CD9-CD41, because two paired antibodies were

detected. In addition, the two pairs CD9-CMDR and CD41-CMDR show comparable colocalization ratio (41% (+/-2) and 38% (+/-4.5)). Notably, staining with CMDR is not as targeted as with use of conjugated antibodies, due ubiquitous binding to all lipid-membrane particles. In contrast to our previous study (see above), we here observe a lower colocalization ratio of CD9-CD41 (58.5% vs. 39%), most probably because a different batch of MSC-EVs was used.

As expected, no colocalization events were observed in the detergent controls using 0.5% NP-40 (see figure 3 D-F).

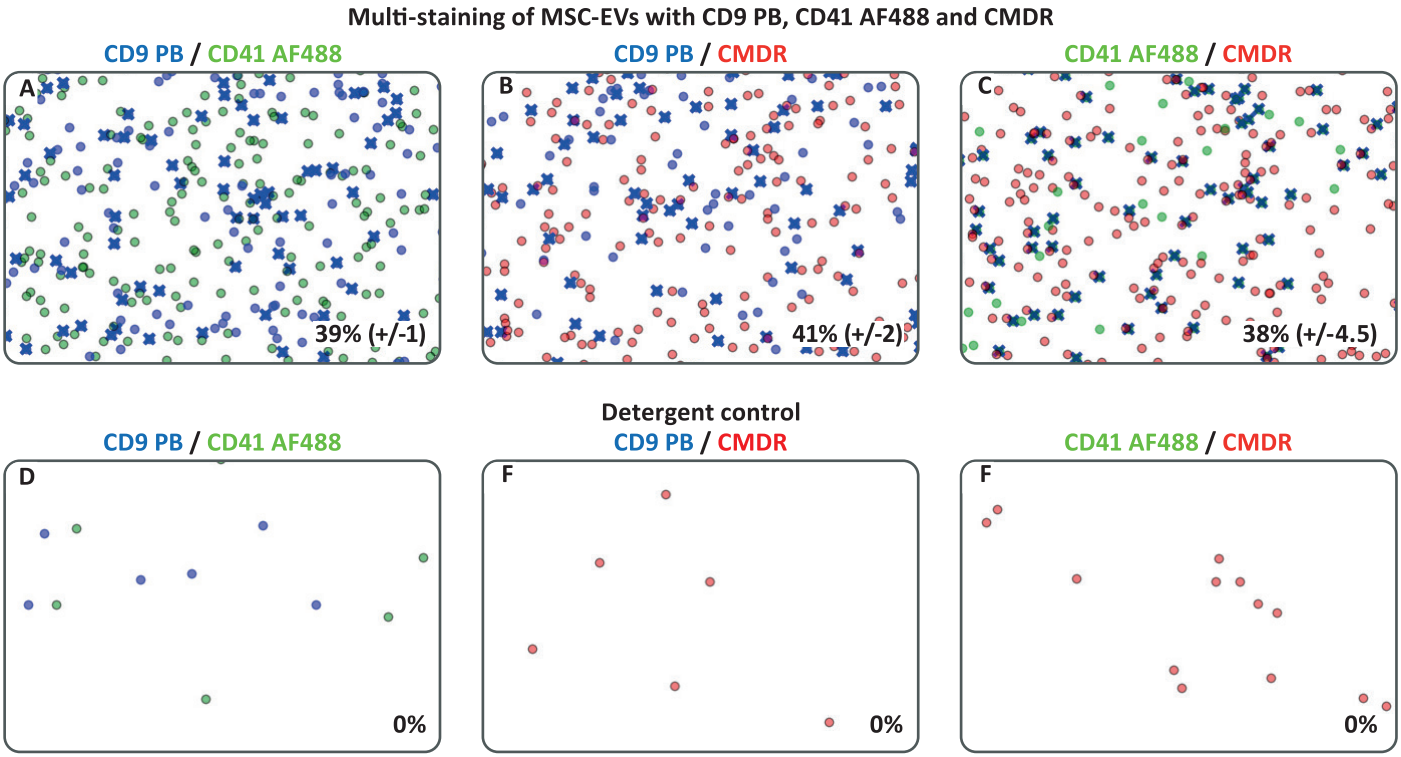

Figure 3: Representative sections of the x-y centroid coordinates of the scattering events of MSC-EVs multi-stained with antibodies against CD9 PB, CD41 AF488 and CMDR and detected in the corresponding pair of fluorescence channels. Each blue, green and red dot represents an EV positive for CD9, CD41 and CMDR, respectively. Double positive events are highlighted by a blue cross and are depicted as percentage in the bottom right of each plot. ***A-C:*** *Colocalization events of EVs detected in the corresponding pair of fluorescence channels.* ***D-F:*** *No colocalization events were observed in the detergent control after addition of 0.5% NP-40 solution.*

Different sequences of EV-labelling:

The more dyes or antibodies that are used for C-NTA, the more diverse the sequence in which the different dyes can be added. In order to investigate whether colocalization ratios are dependent on the order in which the antibodies and mermbrane labels were added, we tested 4 different staining sequences on the MSC-EVs. The result is shown in figure 4 and shows that, at least with this mixture of labels, no significant difference in the colocalization results was observed for the different staining sequences.

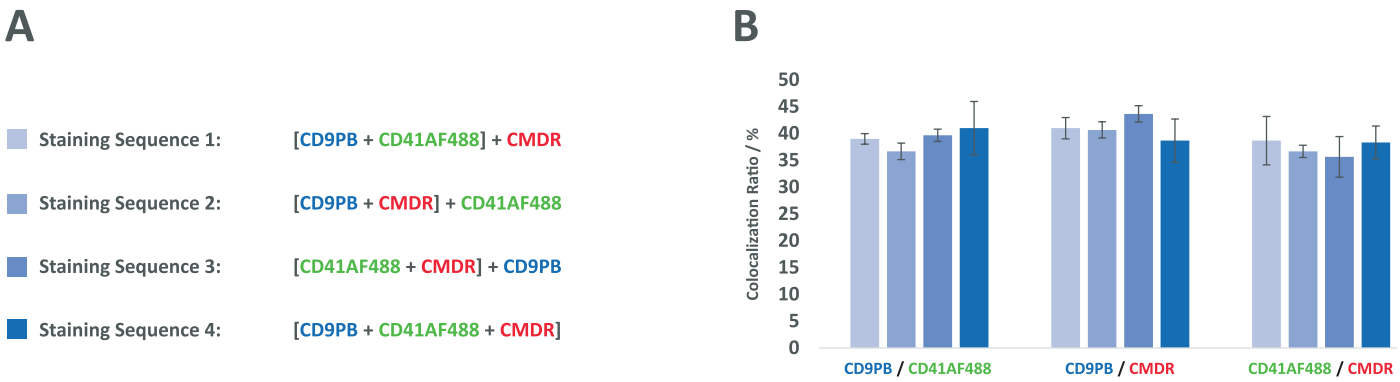

*Figure 4: **A:** Four different staining sequences were investigated for multi-labelling of the MSC-EVs. The labels in the square brackets were first incubated with the MSC-EVs for one hour, followed by the addition of the third label with an additional hour of incubation. Staining sequence 4 was incubated directly for 2 hours. **B:** Dependency of colocalization ratio on different staining sequences.*

FMO-controls:

Fluorescence minus one (FMO) controls are important when identifying a positive from a negative population. When acquiring data, there might be fluorescence spread (spill-over), particularly with brighter fluorophores, which is noticeable after compensation (not required in this study) and cross-laser excitation. FMO controls have been done for all fluorophores in our panel when we started the new multicolor experiment. During staining, one dye or antibody was omitted, but colocalization was still tested in all available fluorescence channels (see figure 5). As a result, depending on the combination of the dyes, there was only one pair of fluorescence channels in which colocalization was observed.

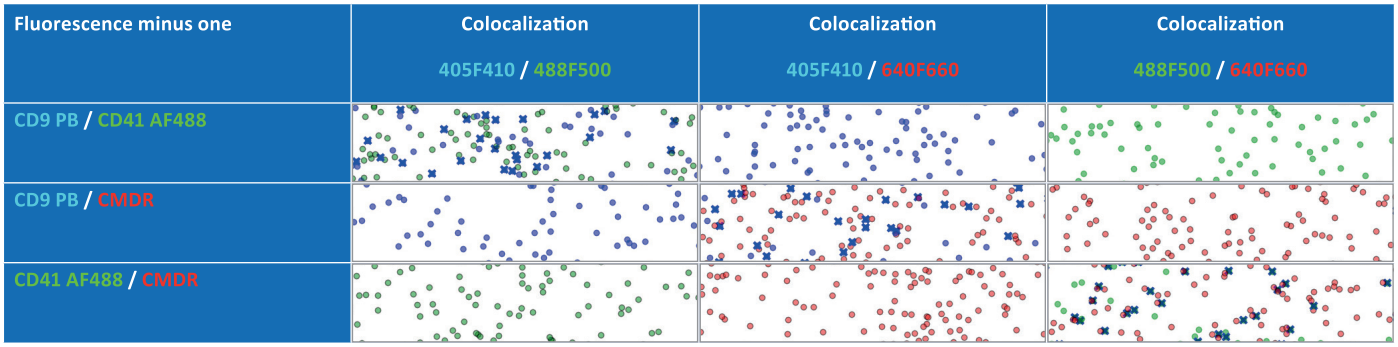

Figure 5: FMO controls on MSC-EVs. The column on the left shows the double staining where the third labelling (antibody or CMDR) was skipped. Columns 2-4 denote respective pairs of fluorescence channels in which the labeled EVs are detected. FMO controls showed colocalization in only one pair of the used fluorescence channels when omitting one fluorophore.

Summary

In this study, we describe for the first time the characterization and phenotyping of multi-labeled EVs using C-NTA. We were able to quickly and reproducibly detect the ratio of CD9/CD41, CD9/CMDR and CD41/CMDR double positive EVs using multiple lasers and flexibly selectable pairs of fluorescence filters. Since brownian motion is also tracked during each C-NTA measurement, accurate size distributions and concentration information of all fluorescent EV-subpopulations are available during a single measurement, simultaneously with the colocalization data.

False-positive detections and artefacts were prevented with the detergent controls. Furthermore,

these controls verified that the colocalized particles were indeed EVs.

FMO controls did not show any fluorescence spread in adjacent channels, thus proving the specificity of both (i) the labeling, and (ii) the fluorophores with regard to the fluorescence channels used. The possible permutations for labelling sequences increase greatly with each additional label, thus we tested different staining sequences and found that the staining sequence has no significant influence on the colocalization ratios examined here.

As in our previous study, negative controls prepared without MSC-EVs, but containing all other components, show a significantly reduced number of particles compared to the positive samples, and the diameter of the particles remained roughly the same (data not shown).

The use of highly targeted C-NTA experiments shows that combinations of antibody and membrane staining can determine the amount of EVs of interest. In addition, C-NTA has proven to be an accurate tool for the detection and identification of biomarkers at the single particle level within a single measurement, including the benefit of accurate sizing and concentration measurement.

C-NTA therefore offers a highly targeted approach to helping unravel the remaining mysteries in the exciting world of EVs.

References

1. **Koliha N, Heider U, Ozimkowski T, et al.:**
   Melanoma affects the composition of blood cell-derived extracellular vesicles [original research]. Front Immunol. **2016 Jul;**7(282). English.
   DOI:10.3389/fimmu.2016.00282

2. **Koliha N, Wiencek Y, Heider U, et al.:**
   A novel multiplex bead-based platform highlights the diversity of extracellular vesicles. J Extracell Vesicles. **2016;** 016;5:29975. PubMed PMID: 26901056; PubMed Central PMCID: PMCPMC4762227.

3. **Wiklander OP, Nordin JZ, O'Loughlin A, et al.:**
   Extracellular vesicle in vivo bio-distribution is determined by cell source, route of administration and targeting. J Extracell Vesicles. **2015**;4:26316. PubMed PMID: 25899407; PubMed
   Central PMCID: PMCPMC4405624.

4. **Wiklander OPB, Bostancioglu RB, Welsh JA, et al.:**
   Systematic methodological eva-luation of a multiplex bead-based flow cytometry assay for detection of extra-cellular vesicle surface signatures
   Front Immunol. **2018 Jun**;9(1326).
   English. doi: 10.3389/fimmu.2018.01326.

5. **Kowal J, Arras G, Colombo M, et al.:**
   Proteomic comparison defines novel markers to characterize heterogeneous populations of extracellular vesicle sub-types. Proc Natl Acad Sci U S A. **2016 Feb 8**. PubMed PMID: 26858453.
   DOI:10.1073/pnas.1521230113.

6. **Giebel B.**
   On the function and hetero-geneity of extracellular vesicles. Ann Transl Med. **2017 Mar**;5(6):150.
   PubMed PMID: 28462230; PubMed Central PMCID: PMCPMC5395490.

7. **Witwer KW, Buzas EI, Bemis LT, et al.:** Standardization of sample collection, isolation and analysis methods in extracellular vesicle research. J Extracell Vesicles. **2013;**2. PubMed PMID: 24009894; PubMed Central PMCID: PMCPMC3760646. DOI:10.3402/jev.v2i0.20360

8. **Sharma S, Rasool HI, Palanisamy V, et al.:** Structuralmechanical characterization of nanoparticle exosomes in human saliva, using correlative AFM, FESEM, and force spectroscopy. ACS Nano. **2010;**4(4):1921–1926.

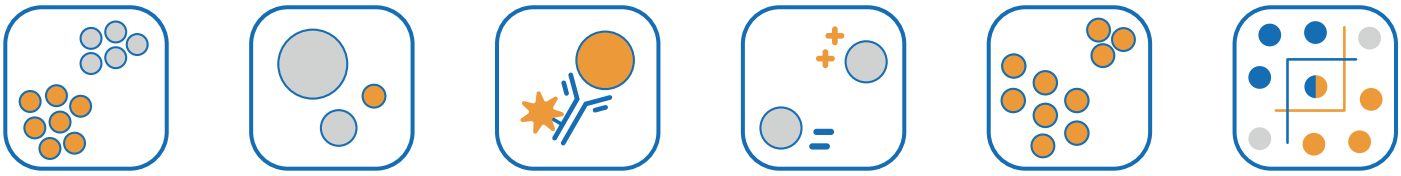

Head Office

Particle Metrix GmbH
Wildmoos 4
D-82266 Inning / Germany

+49-8143-99172-0
info@particle-metrix.de

US Office

Particle Metrix Inc.
Mebane, NC 27302 / USA

+1-919-667-6960
usa@particle-metrix.com

Worldwide Distributors